buildings

MDPI

Review

Effects of Niobium Addition on the Mechanical Properties and Corrosion Resistance of Microalloyed Steels: A Review

André Vitor Benedito [1,*], Carlos Alberto Benedetty Torres [2], Rebecca Mansur de Castro Silva [3], Pablo Augusto Krahl [4,5], Daniel Carlos Taissum Cardoso [6], Flávio de Andrade Silva [6] and Carlos Humberto Martins [1,5]

1 Department of Civil Engineering, Federal University of São Carlos, São Carlos 13565-905, Brazil; chmartins@uem.br
2 Department of Civil and Environmental Engineering, University of Engineering and Technology-UTEC, Lima 15063, Peru; cbenedetty@utec.edu.pe
3 Department of Civil Construction and Transportation, Rio de Janeiro State University, Rio de Janeiro 20550-013, Brazil; beccamansur@eng.uerj.br
4 Department of Civil Engineering, Mackenzie Presbyterian University, Campinas 13073-148, Brazil; pablo.krahl@mackenzie.br
5 Department of Civil Engineering, State University of Maringá, Maringá 87020-900, Brazil
6 Department of Civil and Environmental Engineering, Pontifical Catholic University of Rio de Janeiro, Rio de Janeiro 22451-040, Brazil; dctcardoso@puc-rio.br (D.C.T.C.); fsilva@puc-rio.br (F.d.A.S.)
* Correspondence: andrebenedito@estudante.ufscar.br

Abstract: Steel structures are prone to corrosion, a chemical reaction between steel and the atmosphere that gradually weakens the material. Over time, this reaction can significantly reduce the structural integrity and lifespan of steel elements. Without intervention, corrosion can cause structures to fail, leading to financial, environmental, and potential human losses. Enhancing steel's corrosion resistance is crucial, and one method involves adding niobium (Nb). Niobium microalloyed steels are known for their increased strength, and some research indicates that Nb may also improve corrosion resistance by making the grain structure of the steel finer. However, the complete potential of Nb in corrosion prevention remains underexplored, with significant research gaps across various scales, from microstructural impacts on durability to macroscopic effects on mechanical properties. The research community has utilized numerous experimental approaches to test corrosion resistance under different conditions, but there is a lack of comprehensive studies that aggregate and analyze these findings. This paper seeks to fill that void by reviewing the impact of Nb on the strength and corrosion resistance of structural steels, examining how steel beams' ultimate capacity degrades over time and identifying key areas where further research is needed to understand Nb's role in mitigating corrosion.

Keywords: microalloyed steel; niobium; grain refinement; steel beams

Citation: Benedito, A.V.; Benedetty Torres, C.A.; Silva, R.M.d.C.; Krahl, P.A.; Cardoso, D.C.T.; Silva, F.d.A.; Martins, C.H. Effects of Niobium Addition on the Mechanical Properties and Corrosion Resistance of Microalloyed Steels: A Review. *Buildings* **2024**, *14*, 1462. https://doi.org/10.3390/buildings14051462

Academic Editors: Michael Raupach and Sylvia Kessler

Received: 9 April 2024
Revised: 28 April 2024
Accepted: 7 May 2024
Published: 17 May 2024

1. Introduction

Microalloyed steels are commonly used in several engineering projects mainly due to their excellent mechanical properties, namely high strength and toughness [1]. The applications of microalloyed steels cover several areas, such as the oil and gas industry, structures exposed to the marine environment, and the automotive industry. The literature has reported its specific use for constructing pipelines, offshore platforms, cross-sea bridges, subsea tunnels, port terminals, and railways [2–6]. Such steel structures close to marine atmospheres are exposed to salt spray and, therefore, are susceptible to marine corrosion, which can reduce the structure service life due to the element's thickness reduction, causing degradation of the strength capacity over time.

In terms of the composition, microalloyed steels have low carbon (C) contents, varying between 0.05% and 0.25%, and a manganese (Mn) content of up to 2.0% [7]. Furthermore, small additions of other elements, such as chromium (Cr), nickel (Ni), molybdenum (Mo), copper (Cu), nitrogen (N), vanadium (V), niobium (Nb), titanium (Ti), and zirconium (Zr) can be combined to achieve improved mechanical and durability properties [8]. It is well known that Nb addition improves steel's strength and toughness through the precipitate-strengthening effect that produces grain refinement at the microstructural level [9–13]. Compared to other elements, Nb also presents a lower mass, inducing higher performance. The Nb particles precipitate on the steel substrate, delaying the recrystallization process and promoting non-recrystallization, which results in finer grains [14]. The precipitates act as barriers that hinder the dislocation movement, and thus, more energy is required during the material deformation [9]. According to Zhang et al. [10], a 0.034 wt.% Nb addition can generate grain refinement of up to 71% compared to steels without Nb added. Moreover, Nb also has a more abundant supply than the other elements and a more stable cost, thus being more advantageous as an addition to microalloyed steels [15].

As can be seen, there is a clear understanding in the literature of Nb effects on steel mechanical properties. However, there are still gaps in knowledge regarding the impact and potential of Nb addition on the corrosion resistance of microalloyed steels [16]. Some studies show that small Nb additions can improve steel corrosion resistance in different environments. According to Liu et al. [12], an appropriate amount of Nb addition in microalloyed steels increases corrosion resistance due to a more homogeneous microstructure generated by the precipitation of Nb carbide (NbC). NbC precipitates prevent the accelerated anodic dissolution of steel, improving corrosion resistance [10]. Nam and Kim [17] showed that higher Nb, from 0 wt.% to 0.10 wt.% Nb, lowers the corrosion rate caused by exposure to sulfuric acid. This was attributed to a change in the electrochemical properties of the steel. The Nb-microalloyed steels had higher passive resistance and charge-transfer resistance. A passive protective film, composed of relatively inert Nb oxides, formed on the surface of the steel during the oxidation process, improving the corrosion resistance performance [18]. Wang et al. [19], through surface morphological analysis, observed that the corrosion product films after seawater immersion in steels with 0.079 wt.% Nb addition are more compact than those in the steels without addition. This compaction improves the resistance to the ion migration during the electrochemical reaction, thus reducing the steel degradation velocity caused by the chloride ions.

A literature mapping based on microalloyed steel behavior shows that most studies have focused on the mechanical properties of the material under non-aggressive atmospheres. In contrast, other aspects, such as the corrosion resistance of Nb-microalloyed steels have been less studied. Thus, this paper explores the current state-of-the-art corrosion resistance of Nb-microalloyed steels exposed to corrosive atmospheres. The experimental techniques used to evaluate the degradation of small samples (steel coupons) and large elements (steel beams) are also addressed, and the advantages and disadvantages of these techniques are discussed. The paper exposes the main knowledge gaps on the subject and reinforces the advantages and potential of Nb as an addition to steel alloys, aiming at constructing structures with greater mechanical resistance and durability.

2. Effects of Nb on Microalloyed Steels

2.1. Effects at the Microstructural Level

Nb, Ti, and V are the most commonly used microalloying elements to improve steel mechanical properties [20–22]. These elements are combined with C and nitrogen (N) during the manufacturing processes to promote the formation of precipitates responsible for increasing the strength and hardness of the steel [23,24]. Nb, for example, presents elevated affinity with C and N, facilitating the formation of Nb(C, N) carbonitride's that contribute to strengthening the steel matrix [25]. Some studies suggest that smaller amounts of Nb addition, compared to Ti and V, can promote more significant increases in the yield and ultimate strength [15,26]. Rancel et al. [26] compared the influence of additions of 0.019 wt.% Nb, 0.038 wt.% Ti, and 0.070 wt.% V on the steel yield strength, and the Nb-microalloyed steel exhibited a yield strength of 30 MPa and 80 MPa higher than the Ti and

V-microalloyed steels, respectively. This aspect makes Nb a more interesting microalloying element to improve steel performance.

Nb addition to steel can mainly affect the microalloyed steel solidification process; for example, the Nb present in steel in the form of Nb-containing phases and Nb solute promote ferrite and bainite formation, respectively. Ferrite benefits toughness and plasticity, while bainite affects strength and hardness [15]. Furthermore, grain boundaries influence the material mechanical properties in polycrystalline materials, such as steel. The discontinuities and orientation differences between the slip planes of each grain promote movement restriction [27]. The increase in the Nb content in the steel induces a reduction in the grain size (see Figure 1a), consequently producing a decrease in the dislocations per grain [28]. This effect makes the movement between adjacent grains even more difficult, thus generating what is known as grain boundary strengthening [29], as shown in Figure 1b. Another strengthening mechanism is related to the Nb solute atoms (see Figure 1c). The presence of Nb atoms in the crystal lattice generates localized defects that distort and hinder movement at the atomic level [15]. Stress fields arise in the proximity of the Nb atoms, deforming the crystal lattice in localized regions that hinder free movement [30].

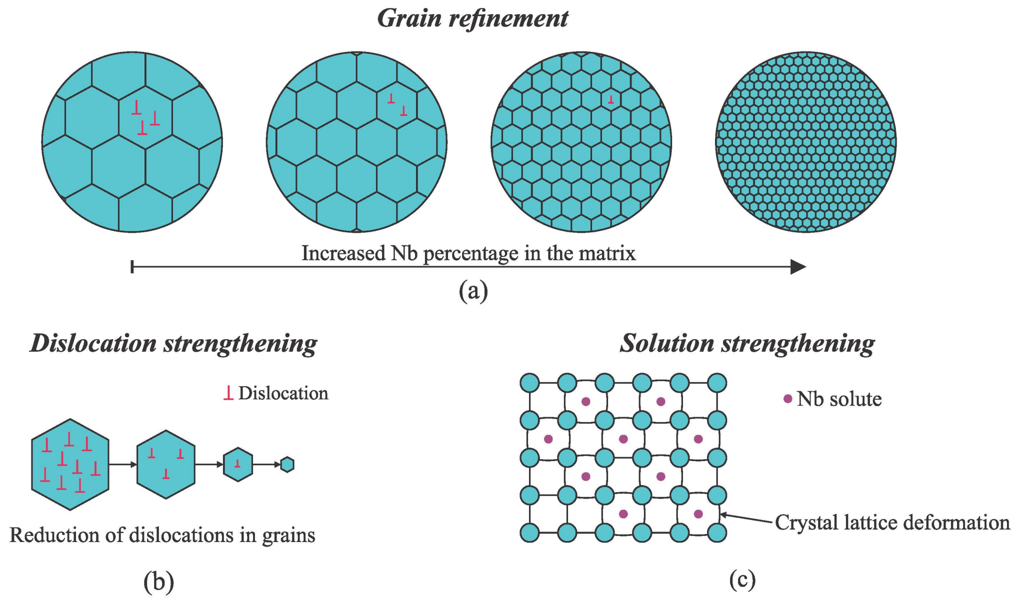

Figure 1. Strengthening mechanisms due to Nb addition: (**a**) grain refinement, (**b**) dislocation strengthening, and (**c**) solution strengthening.

When Nb is incorporated into steel, it undergoes non-uniform dispersion among the iron atoms and other alloying elements constituting the steel matrix. This dispersion phenomenon significantly contributes to the formation of Nb solutes, thereby exerting discernible effects on the mechanical attributes of the steel. Niobium solutes impede grain mobility via a mechanism recognized as solute drag, wherein the solute atoms impede the motion of metal atoms during deformation processes. Throughout this mechanism, Nb solutes effectively impede the migration of grain boundaries, consequently engendering enhancements in mechanical properties. Moreover, the formation of niobium carbides during the heat-treatment procedures of steel also confers enhancements in mechanical characteristics. Due to the high hardness and stability of Nb carbides, they instead act as physical barriers that improve the wear and abrasion resistance.

2.2. Grain Refinement Impact on the Steel Mechanical Properties

The mechanism through which the added Nb refines the grain size of the steel is related to the formation of nucleation sites during the matrix manufacturing process. Nb is an element that, owing to its chemical properties, exhibits a high affinity for oxygen and sulfur, resulting in the formation of niobium oxides and sulfides during the steel solidification process. These compounds serve as nucleation sites within the matrix, promoting the formation of additional austenite grains, a crucial iron phase for the mechanical properties of steel. Additionally, the nucleated particles act as physical barriers that hinder grain movement during material deformation. Similarly, niobium atoms can interact with the dislocations, affecting their mobility and anchoring capacity. Other compounds can also form during steel manufacturing; for instance, during the heat treatment process, niobium carbides are formed and dispersed throughout the matrix. Carbides exert a different influence on grain boundary mobility due to their higher hardness compared to niobium oxides and sulfides. In this scenario, the steel can exhibit enhanced mechanical properties, as it offers greater resistance to dislocation sliding.

The alterations produced in the steel microstructure and steel composition due to the Nb addition are commonly analyzed using microscopy and spectroscopy techniques. Among the most used techniques to analyze the metallographic microstructure are optical (OM), scanning electron (SEM), and transmission electron (TEM) microscopy [19,31,32]. Other aspects, such as the grain boundary misorientation and the crystallographic size, can be quantified through the Electron Backscatter Diffraction (EBSD) technique [3,4,11,16,33,34]. On the other hand, when it is required to know the elemental composition, Energy Dispersive Spectroscopy (EDS) or the Optical Emission Spectrometer (OES) are used [2,12,13,18,32,35–40]. Zhang et al. [10] evaluated the microstructure of high-strength steels with 0.00 and 0.03 wt.% Nb. Microstructure images obtained using an optical microscope are presented in Figure 2. An austenitic grain-refinement effect was observed due to the Nb addition. However, the increase in tensile strength was only 0.76%. Zong and Liu [41] studied the Nb influence on the yield strength, ultimate tensile strength, and elongation of Ultra-Low Carbon Bainite (ULCB) steel. The Nb content added was 0.035 wt.%, 0.069 wt.%, 0.084 wt.%, and 0.107 wt.%. The steels showed improvements in the yield strength and ultimate tensile strength compared to steel with 0.035% Nb. The maximum increases achieved were 9.46% and 5.88%, respectively, substantially greater than those reported by Zhang et al. [10]. However, the steel elongation was impaired for some additions greater than 0.035%, suggesting a possible ductility loss due to the Nb addition. The refinement of the microstructure can reduce material ductility while increasing its strength. Among the additions evaluated by Zong and Liu [41], 0.069% Nb was shown to be an optimal value for strength and elongation.

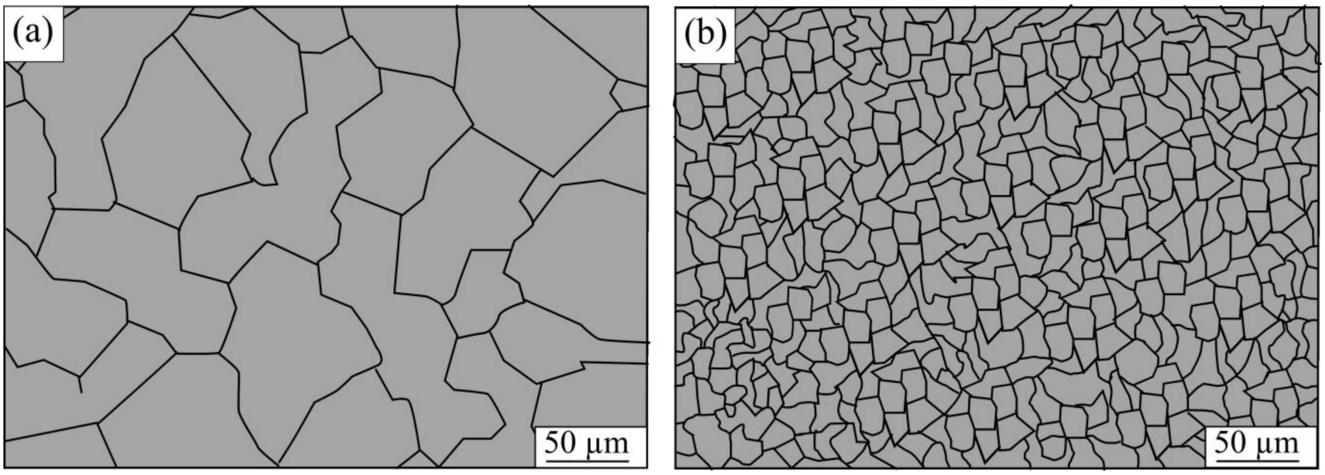

Figure 2. Austenite grain of steels with (**a**) 0.00 wt.% Nb and (**b**) 0.03 wt.% Nb. Adapted from Zhang et al. [10].

Jack and Szpunar [16] observed a similar effect to that reported by Zong and Liu [41] where the steel elongation and, consequently, the ductility were affected by increasing the Nb content from 0.008 to 0.080 wt.%. Figure 3a shows that the sample with the highest Nb content presented the highest yield strength and ultimate strength; however, it failed with significantly less strain without showing a yield plateau. These results indicate that the grain-refinement effect has a more significant beneficial impact on the yield strength, ultimate strength, and toughness than on the ductility and strain capacity [31]. However, an opposite finding was reported by Tian et al. [11] when comparing ultra-high-strength stainless steel without Nb and with a high Nb content (0.11 wt.%); they observed that the latter presented lower plasticity and ultimate tensile strength. The authors associated this detriment in mechanical properties to the high Nb content, resulting in large particles corresponding to a second undissolved phase on the steel matrix. The particles interrupt the matrix continuity and induce stress concentration during deformation. This stress concentration leads to a worsening of plasticity and tensile strength.

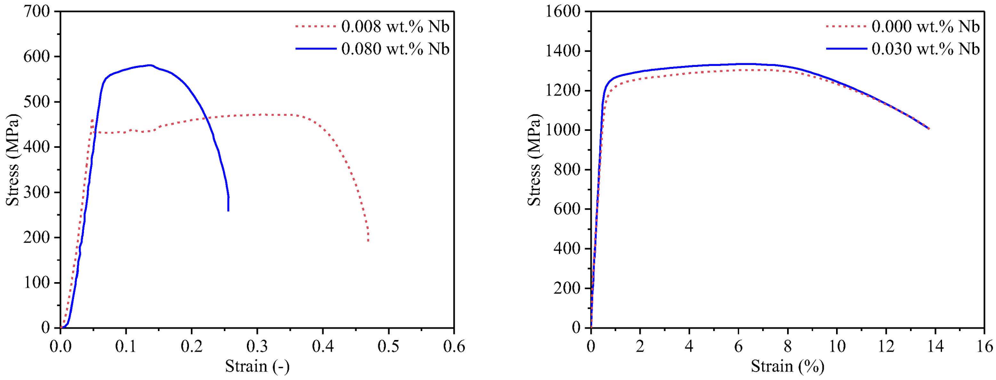

(**a**) (**b**)

Figure 3. Effect of Nb content on the stress–strain response of (**a**) normal-strength Adapted from Jack and Szpunar [16] and (**b**) high strength-steel. Adapted from Zhang et al. [10].

On the other hand, studies show that the fact of adding Nb will not necessarily generate a decrease in ductility. In addition to the added Nb content, other aspects, such as the steel strength and its chemical composition, can influence the ductility. For example, the stress–strain curves obtained by Zhang et al. [10] (Figure 3b) indicate that the addition of 0.030 wt.% Nb did not negatively affect ductility in high-strength V-microalloyed steels. Likewise, the effects on increasing strength and toughness were not significant. The main benefits of the Nb addition were a decrease in the corrosion rate by 24% and a 13% lower susceptibility to hydrogen-induced delayed fracture (HIDF). Both effects were promoted by grain refinement and hydrogen trapping induced by NbC precipitates [42]. Another study developed by Wu et al. [3] found a similar trend. In this case, the mechanical properties of high-strength steel were not significantly affected by adding 0.06 wt.% Nb. Properties, such as the yield and ultimate strength suffered reductions of just 3.05% and 1.07%, respectively. Meanwhile, the steel elongation presented an increase of 5.71%.

2.3. Effects on Cyclic Mechanical Behavior

Although several investigations show the benefits of Nb addition in steels subjected to quasi-static loading, a few studies have explored the behavior under cyclic loading. Zhao et al. [43] analyzed the behavior of Nb-microalloyed steels subjected to ultra-high fatigue cycles (109 cycles). A parameter evaluated in the study was the ratio of fatigue limit to the tensile strength measured under quasi-static conditions. It was found that Nb-microalloyed steels develop ratios of approximately 0.55, which is higher than that observed in other high-strength steels without the Nb addition. The increase in the fatigue limit is attributed to the grain refinement mechanism caused by the Nb addition. Finer grains promote a decrease in the stress concentration in their boundaries, impacting improvements, such as more uniform deformation and increased fatigue strength. According to Zhao et al. [44], Nb(C, N) carbonitride particles induce a pinning effect that reinforces the matrix at a microstructural level. In this way, the resistance to high-fatigue cycles is improved since the particles inhibit plastic deformation.

On the other hand, studies that have evaluated the effects of corrosion and cyclic loading in Nb microalloyed steels are more scarce. A study developed by Xu et al. [42] is one of the few that has explored the effects of the addition of Nb on the corrosion fatigue behavior of high-strength steels. The authors found that adding 0.1 wt.% Nb can reduce the susceptibility to marine corrosion fatigue by 8%. However, the most notable beneficial effect was when high-strength steel was subjected to a hydrogen charging environment, such as pressure vessels and pipelines. The corrosion fatigue sensitivity in these cases can be reduced by up to 40%. According to the authors, the steel microstructure refinement and the formation of NbC precipitates inhibit the nitrogen concentration, promoting steel embrittlement. In this way, the initiation and propagation of cracks is minimized.

2.4. Effects on Corrosion Resistance

The corrosion of steel structures is a significant issue that leads to the deterioration and failure of infrastructure components, resulting in enormous economic losses and potential safety hazards. Niobium has shown great potential in preventing the corrosion of microalloyed steels, especially in corrosive environments. Several studies have investigated the effect of the niobium content on the corrosion resistance and durability of steel structures [9,12,17,40,45–48].

The literature has reported two strategies to improve steel corrosion resistance using Nb. The most common practice is adding Nb to the steel composition during manufacturing. The other less explored strategy involves applying an Nb-based coating to the steel surface [12,45]. In both cases, the added Nb content is crucial, so it should be defined based on the steel characteristics and the aggressiveness of the corrosive atmosphere.

The parameter commonly used to evaluate corrosion resistance is the corrosion rate, frequently expressed in millimeters per year. This parameter is indirectly determined since it is necessary to experimentally quantify other variables, such as the mass loss or thickness reduction. The corrosion rate can also be determined from electrochemical techniques, for example, via the potentiodynamic polarization technique [46]. In the literature, various corrosive environments have been evaluated, including sulfuric acid, NaCl, and CO_2-polluted saline atmospheres. Specifically, Nam and Kim [17] assessed the effects of adding 0.05 and 0.10 wt.% niobium on the corrosion resistance of low-alloy steel exposed to a 10 wt.% sulfuric acid solution. It was found that increasing the Nb content promotes the decrease in the passive current within the corrosive environment. The researchers attribute this tendency to the fact that the Nb present in the steel creates an oxide layer that protects its surface, thus inhibiting the steel dissolution. The addition of 0.05 and 0.10 wt.% Nb reduced the corrosion rate by 28% and 54%, respectively (see Figure 4).

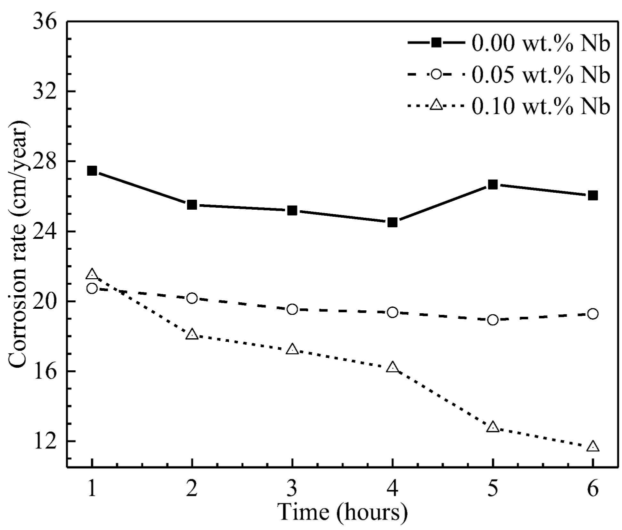

Figure 4. Influence of Nb addition on the corrosion rate of low-alloy steels exposed to sulfuric acid. Adapted from Nam and Kim [17].

The Nb effects on the corrosion resistance induced by hydrogen sulfide (H_2S) were studied by Liu et al. [9]. The H_2S solution was prepared by injecting distilled water into an autoclave, and then, nitrogen with 99.99% purity was injected to eliminate oxygen from the solution. To maintain the properties of the solution, H_2S was continuously injected into the autoclave during the immersion of the samples. Surface micrographs of steels with 0.00 and 0.07 wt.% Nb captured after 240 h of immersion in hydrogen sulfide are presented in Figure 5. An analysis of the morphology and composition of the corrosion products suggests that the addition of Nb retards the precipitation rate of corrosion products (iron sulfides). Additionally, a more significant amount of pyrrhotite accumulates on the steel surface. These characteristics contribute to the fact that the porosity of the oxide layer is lower in Nb-microalloyed steel. In fact, a dense and compact layer improves corrosion resistance. In another study, Li et al. [47] exposed steels (0.055 wt.% Nb) with and without hydrogen to electrochemical corrosion in a 3.5% NaCl solution. It was observed that the corrosion resistance improves remarkably only in hydrogen-contained steels. The authors attributed this fact to the hydrogen-trapping effect promoted by the NbC precipitates, which restrict the activation of hydrogen that would accelerate the steel anodic dissolution.

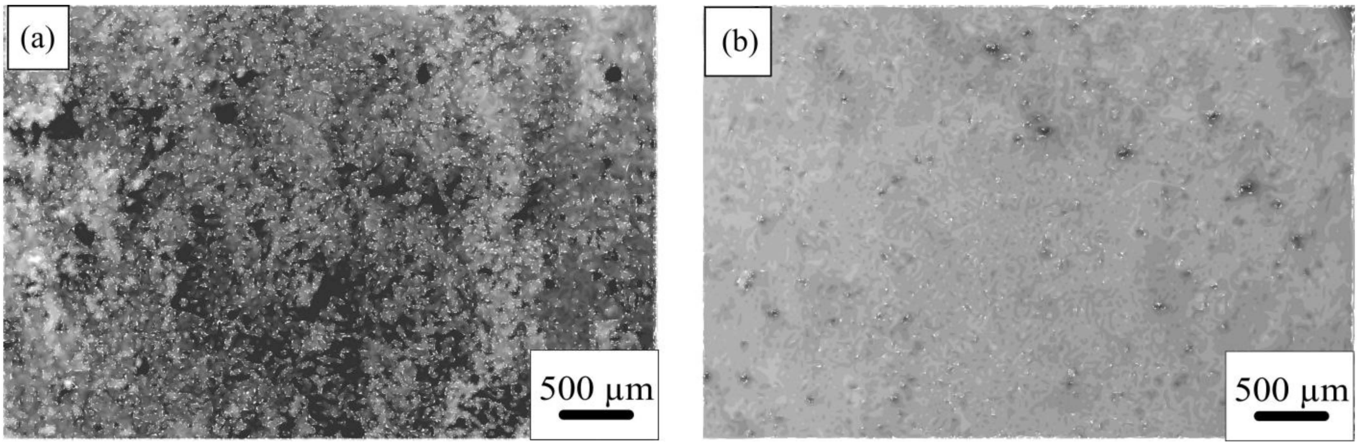

Figure 5. Corrosion products on the surface of the (**a**) Nb-free steel and (**b**) Nb steel samples after 240 h of immersion in H_2S. Adapted from Liu et al. [9]; the figure was vectorized using the free software Inkscape [49].

Liu et al. [12] evaluated the effects of a wide range of Nb additions (0.2, 0.5, 1.0, 3.0, 5.0, and 7.0 wt.%) to a stainless steel coating. Carbon structural steel plates with $100 \times 40 \times 8$ mm dimensions were coated and exposed to electrochemical corrosion using a 3.5 wt.% NaCl solution. It was found that the addition of 1.0 wt.% Nb produced the best performance in terms of corrosion resistance. However, for higher addition values, the performance was lower. It is usually expected that the Nb oxides will accumulate on the steel surface during corrosion, forming a protective film. However, when the added Nb content is excessive (>1.0 wt.%), the formation of Laves phases of ferroniobium (Fe_2Nb) is promoted, making the steel more susceptible to corrosion. In addition, Wu et al. [40] evaluated the influence of Nb and Antimony (Sb) addition on the susceptibility to cracking due to the combined effects of tensile stresses and corrosion in steels. A marine atmosphere polluted by SO2 was simulated in the laboratory to corrode the specimens. It was found that the susceptibility to cracking decreases when adding these elements. Parameters, such as elongation losses and specimen area reduction, measured through slow strain rate tension (SSRT) tests, presented maximum reductions of 57.45% and 37.25%, respectively. The best performance was achieved for addition values of 0.06 wt.% Nb and 0.1 wt.% Sb. According to Wu et al. [40], the performance improvements are because the NbC precipitates reduce the hydrogen available in the steel, decreasing the susceptibility to hydrogen embrittlement. This phenomenon leads to improvements in the microstructure and, consequently, in the strength of steels with respect to cracking due to the combined effects of tensile stresses and corrosion.

3. Mechanical Behavior of Corroded Steel Beams

Since corrosion is a degradation process that occurs gradually over the years, the mechanical properties are also continuously degraded over time. Therefore, it is essential to understand and characterize this degradation behavior directly related to the corrosion level to which the structural element is submitted.

The mechanical property degradation of steel can be analyzed through several methodologies. In general, more corrosion studies on small specimens have been reported in the literature. On the other hand, studies on large-scale specimens, such as beams [48,50–55], columns [56], beam–column joints [57–60], and frames [61], are more scarce [62]. The techniques used to induce corrosion can be classified according to the environment where the corrosion occurs, such as indoor [63] or outdoor [61,64,65] environments. In outdoor corrosion environments, the steel is exposed to the actual conditions of the corrosive atmosphere [64,65]. Uncorroded specimens can be submitted to an in situ corrosion condition. For example, Zhu et al. [65] investigated the corrosion behavior of stainless steel and Ni-alloy samples immersed in the South China Sea. Moreover, it is also possible to evaluate the corrosion resistance of corroded elements and structures. Tzortinis et al. [48] analyzed the mechanical behavior of corroded I-beams from two steel bridges in service since 1939.

The corrosion rate is another variable used to classify corrosion, which means that the corrosion can be induced naturally [48], as in the case of most outdoor corrosion, or induced in an accelerated process [60,62]. The outdoor natural corrosion is advantageous since it is possible to know the real steel corrosion resistance in a specific environment. However, the test duration may become excessive [66] since corrosion is time-dependent.

According to ISO 9223 [67], the environments are classified into six categories based on their ability to induce corrosion in steel and other metals. Specifically, the ISO-C3 and ISO-C4 categories, defined in the standard [67], detail corrosion rates of 25–50 μm/a and 50–80 μm/a, respectively. Zhang et al. [61] report that 18.1–36.3 years of corrosion typical of an ISO-C3 environment can be simulated by 20–120 days of accelerated corrosion using an NaCl solution spray with a concentration of 50 ± 5 g/L and a pH of 6.5–7.2. Similarly, the same conditions can simulate 11.3–18.1 years of corrosion in an ISO-C4 environment. Under laboratory conditions, the degradation process can be accelerated through several techniques, such as immersion in chloride solution, without [68] or with an imposed electric current (electrochemical accelerated corrosion) [69,70], immersion in an acid solution (sulfuric) [17], and exposure to salt spray through cabinets [60]. Although the accelerated corrosion tests do not reproduce the real conditions of the corrosive atmosphere, they allow for an evaluation of the corrosion resistance in a short time [71].

The steel composition affects the mechanical properties of steel corroded beams. On a material scale, Rahbar and Zakeri [68] observed that, in the early stages of accelerated corrosion (first 48 h), the corrosion resistance of high-strength steels (0.003 wt.% Nb) is higher for steels with a higher Manganese (Mn) content, i.e., the specimens with more Mn in their composition presented a lower weight loss. Moreover, compared to normal-strength steel, the decrease in the tensile strength of the high-strength steel is accelerated after 144 h of induced corrosion. It is difficult to perform a comparative analysis of the results available at the structural level since the studies carried out with different types of steel have evaluated different corrosion levels achieved using diverse accelerated corrosion techniques. In this way, it is not trivial to identify the effects of Nb incorporation on the structural behavior of corroded high-strength steel beams. Nevertheless, a discussion on how these parameters can affect the mechanical behavior of corroded steel structures will be performed, regardless of Nb addition. Table A1 (Appendix A) presents a database of the available literature on the corrosion results of microalloyed steel beams with niobium.

Corrosion leads to a reduction in the cross-sectional area of steel beams, as noted in references [70,72–74]. According to Peng et al. [70], at the initial stages of corrosion, or with low levels of corrosion, this reduction occurs in a more random manner, resulting in significant variations in the cross-sectional area along the beam's length. As corrosion progresses, the variation in this parameter tends to stabilize along the length of the beam, likely due to the gradual coalescence of corrosion pits [74]. Xiao et al. [74] found that at lower levels of corrosion damage, the depth of corrosion pits is quite uniform, meaning that the pits are nearly the same depth. However, as corrosion damage increases, the depth distribution of these pits broadens. Furthermore, the extent of variation in the cross-sectional area can influence the beam's slenderness ratio, potentially altering the classification of its flange and/or web. This could also impact the design method and failure mode; for example, local buckling of the compression flange may occur before the global failure [72]. This effect is presented in Appendix A.

Corrosion degradation significantly impacts the load-bearing capacity of steel beams, as demonstrated by Peng et al. [70] and Xiao et al. [74], which both conducted similar tests on high-strength Q460D steel containing 0.19 wt.% Nb (refer to Table A1 in Appendix A). These studies confirmed a direct relationship between the extent of corrosion and the reduction in mechanical properties. Notably, both reported changes in the failure mode of the beams, attributing these changes to corrosion-induced modifications in the slenderness of the web and flange. Despite the use of similar materials, the studies noted markedly different outcomes. Reference [74] observed that a 15% loss in mass due to corrosion led to significant openings in the web, causing a sharp decrease in the peak load by 64.15%. Conversely, [70] found a more modest reduction in the peak load of 32.90%, highlighting the variable impact of corrosion on the structural integrity. Comparing studies [70,74], there is evidence suggesting that steel with a lower niobium content experiences a more pronounced reduction in strength and a higher likelihood of changes in failure patterns with less advanced corrosion effects. However, research comparing the effects of corrosion on beams containing niobium is limited, indicating that the true structural-scale influence of niobium requires further investigation.

4. Effects of Corrosion on Weld Integrity

Steel structures frequently have the significant presence of severe corrosion during their service life [75,76]. In such cases, the weak points in the structure often lie at the welded joints, and when subjected to these loads and corrosion, they can increasingly become a significant contributing factor to structural damage [77]. Consequently, it is important to understand the performance of welds and, within the context of this study, explore the potential for enhancement through Nb addition. Therefore, in welding processes, two crucial areas that significantly impact the mechanical properties of the final product are the weld itself and the heat-affected zone (HAZ), the latter being the region of the metal that, while not melted during the welding process, has experienced changes in its microstructure and properties due to the heat of welding. The microstructure of the HAZ plays a vital role in the mechanical properties after weld fabrication, with welding-induced thermal cycles precipitating phase transitions that catalyze profound alterations in these properties. Such changes include the emergence of harder microstructures, like martensite, which enhance strength while concurrently reducing ductility [78].

Moreover, the peak thermal conditions and the rate of cooling within the HAZ are critical; rapid cooling can yield a refined grain structure, generally increasing toughness but potentially introducing more brittle phases [79]. In addition, the distinct microstructural attributes within the HAZ are crucial for determining the fatigue life of the weldment, with areas of fine grains offering superior fatigue strength compared to their coarser-grained counterparts [80]. Several factors influence the HAZ, including the steel composition, the characteristics of austenite grain coarsening, plate thickness, and welding conditions [81]. These factors can alter properties, such as toughness and susceptibility to cracking [78,79,82]. The HAZ, illustrated in Figure 6, is commonly classified into five distinct regions: the base metal (BM), the tempered zone (TZ), the intercritical HAZ (ICHAZ), the fine-grained HAZ (FGHAZ), and the coarse-grained HAZ (CGHAZ) [83].

Regarding mechanical properties, the CGHAZ and the ICHAZ exhibit the lowest toughness among the different regions of the weld joint [19,84,85], because these areas undergo significant microstructural transformations during the welding process. In the CGHAZ, the high heat input can cause the austenite grains to coarsen significantly [86], while the ICHAZ is subject to complex thermal cycles that can form brittle phases, such as martensite [87]. Increasing the Nb content can improve the toughness, tensile strength, and yield strength of the CGHAZ and ICHAZ due to the microalloying effect that it imparts on the steel matrix [6,13,88]. Additionally, Nb can reduce the grain size and increase the amount of acicular ferrite in the microstructure, improving fracture toughness and plastic deformation resistance, illustrated in Figure 3 [2,6,13,19,88,89].

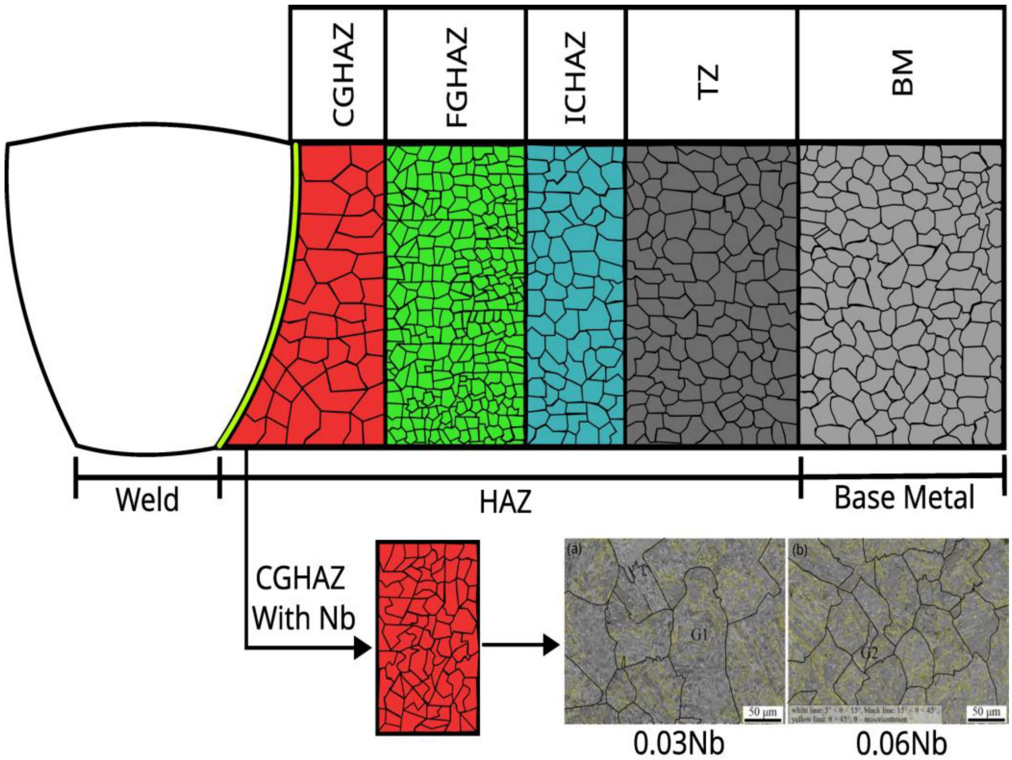

Figure 6. Influence of Nb on the HAZ adapted from Sun et al. [88].

Moreover, Nb segregation at grain boundaries (GBs) can inhibit the initiation and propagation of cracks, as shown in [90]. This paper compared the grain boundary characteristics of pure nickel steel with a nickel-niobium alloy (Ni-0.4Nb), concluding that the presence of stacking faults (SFs) in the Ni-0.4Nb system acts to delay the onset of cracking; these SFs are crystal defects in face-centered cubic materials that disrupt the regular stacking sequence of atomic planes, altering mechanical properties and impeding dislocation motion [91], as illustrated on Figure 7. Nb can also form Nb(C, N), which can act as nucleation sites for acicular ferrite formation [88]. The evaluation of grain sizes in the HAZ requires the use of SEM [2,6,13,88,89], while toughness is determined through the Charpy V-notch impact test [2,6,88,89], following standards, such as ASTM E23-12a [92] and BS EN 10045 [93].

Additionally, the HAZ demonstrates higher susceptibility to corrosion than the BM, where the corrosion resistance in descending order was the BM, TZ, FGHAZ, ICHAZ, and CGHAZ [19,84,94], which can be attributed to the microstructural changes induced by the welding heat [94]. Few articles explore the Nb influence on the corrosion-exposed HAZ. Qiao et al. [13] compared the HAZ of Nb-free and Nb-bearing steel under corrosion. A hydrogen electrochemical charging test was performed to evaluate the material's susceptibility to hydrogen-induced stress corrosion cracking and, simultaneously, a slow strain rate tensile (SSRT) test was conducted to evaluate the mechanical properties of steel.

The research shows that adding Nb reduced vulnerability to stress corrosion cracking in hydrogen-rich environments by acting as a hydrogen trap, limiting hydrogen ingress into the steel. Nanosized NbC precipitates served as permanent traps, reducing the likelihood of hydrogen-induced cracking and enhancing resistance to stress corrosion.

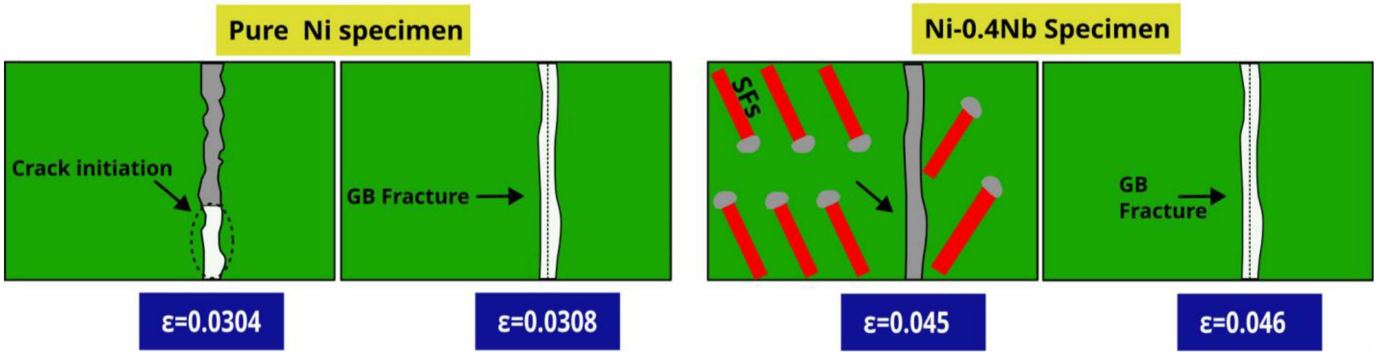

Figure 7. Influence of Nb at grain boundaries. Adapted from Jha et al. [90].

Additionally, the presence of Nb helped decrease grain size and promote consistent fine microstructures, further improving resistance to stress corrosion. Wang et al. [19] investigated the comportment of HAZ on Nb-free and Nb-bearing steel in a simulated seawater solution with electrochemical experiments. Three electrochemical methods were utilized for the measurements: open circuit potential, electrochemical impedance spectroscopy, and potentiodynamic polarization tests. While the standards used for these tests were not explicitly mentioned in the paper, commonly employed standards include ASTM G5 [95] for potentiodynamic polarization tests, ASTM G59 [96] for EIS, and ASTM G102 [97] for OCP measurements. The microstructures of the specimens were observed using OM, a stereo microscope, and high-resolution TEM. The authors concluded that the Nb-bearing samples had more compact and firm corrosion product films than the Nb-free samples. These thin layers of compounds form on the surface of a metal when it corrodes and act as a natural defense mechanism, establishing a barrier between the metal and the corrosive environment through the composition of various corrosion products, like oxides, hydroxides, and salts [98]. The integrity and compactness of these films are crucial in determining the metal's corrosion resistance, with more compact films offering greater resistance to ion migration and thus diminishing the extent of corrosion-induced destruction [99]. The enhanced compactness of the corrosion product films on the Nb-bearing samples bolstered their resistance to ion migration, effectively inhibiting the initiation and propagation of pitting holes caused by the chloride ion. Consequently, the corrosion resistance of the Nb-bearing steel was significantly improved. Consequently, this hindered the onset and spread of pitting damage caused by chloride ions, as shown in Figure 8. The corrosion current density and the corrosion potential were lower in Nb-bearing steel. Both studies conclude that Nb-bearing steel tensile strength and yield strength after corrosion were higher than Nb-free steel's, and the Nb inclusion in the steel improved the strength and corrosion resistance of the welded joints in the Nb-bearing steel's. This enhancement can be attributed to the nanosized precipitation, uniform microstructures, and other associated effects of adding Nb as a microalloy [13,19]. Besides these findings, variations in the composition and microstructure between the HAZ and the BM can cause localized differences in electrochemical potential, thereby promoting galvanic corrosion [77].

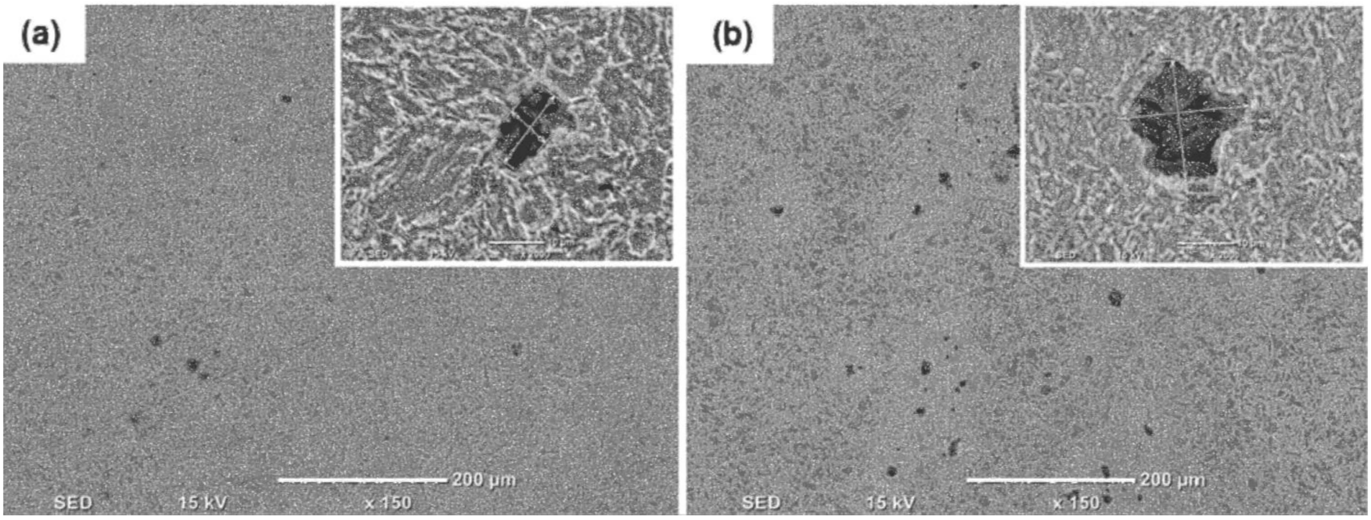

Figure 8. Pitting corrosion on ICHAZ for (**a**) Nb-bearing and (**b**) Nb-free steels immersed in seawater. Adapted from Wang et al. [19]; the figure was vectorized using the free software Inkscape [49].

5. Current Challenges and Future Research Needs

The article discusses the advantages of incorporating niobium into steel, emphasizing its significant impact on enhancing strength, toughness, and corrosion resistance. Niobium improves steel's grain structure, which in turn boosts mechanical properties and resistance to environmental degradation. It also forms niobium carbides that protect steel in corrosive environments and fosters a more uniform microstructure, reducing the steel's vulnerability to issues, like pitting and stress corrosion cracking. The effectiveness of niobium depends on its concentration, necessitating tailored optimization based on specific environmental conditions and application requirements. The article underscores the importance of ongoing research to precisely adjust niobium's use in steel, highlighting that there are still challenges to overcome and new research needed, which are detailed in the following sections.

- Although several studies have explored the impact of Nb addition on the mechanical properties and corrosion resistance of microalloyed steels, the improvement in properties and a subsequent deleterious effect as the percentage of Nb increases suggests the existence of an optimal percentage for each type of alloy. Future studies can be conducted to identify optimal additions for structural additions that could be subjected to high loads and corrosive environments.
- Although the positive influence of Nb addition on the mechanical properties of steels is widely known, studies elucidating the effects of Nb addition on steels exposed to salt spray are quite limited. Experimental investigations must be conducted to identify the optimal Nb addition percentages that would generate better mechanical and durability performance. The results of these studies can be applied to the production of Nb-microalloyed steels for structures exposed to the marine atmosphere.
- As discussed throughout the paper, several factors, such as the corrosion level, corrosion rate, and steel composition, influence the mechanical behavior of corroded steel structures. There is no standard for evaluating the properties affected by the corrosive process, and each study considers different scenarios and variables. Therefore, it is a challenge to compare different studies and evaluate the contribution of each factor in the residual properties of corroded elements, aiming to establish the best material solution for each design configuration.
- As discussed throughout the paper, corrosion in the welded joints is important for structural behavior, as it can be the weakest region for corrosion. In this regard, no studies addressing alveolar beams under corrosion were found during the information-gathering process. In these beams, the cutting and welding process is typically applied to increase the structural performance. Conducting studies to assess its corrosion resis-

tance and exploring potential methods to enhance its performance, such as utilizing Nb, are of paramount importance.
- Some relevant aspects have not been investigated yet. The phenomenological changes in microstructure are achieved by adding Nb to the material nonlinear hardening behavior. Also, cyclic test results to understand hysteresis, which are fundamental to applying or developing constitutive models, can buster the investigations on a meso and macroscale and promote the material application.
- No investigation was found on Nb-microalloys submitted to stress states in aggressive environments, which is essential for other steel types, like stainless steel [100]. Such an investigation represents the actual condition of the structural elements and is necessary for expanding the use of such alloys.
- The literature mapping revealed that there are no studies that evaluate the influence of temperature corrosive environments on the mechanical property degradation of Nb-microalloyed steels. Future studies could be developed on this topic through the use of temperature-controlled salt spray chambers.

6. Conclusions

- While some standards prescribe a limit addition value of 0.07 wt.% Nb, the experimental studies reviewed provide evidence that higher addition values can significantly enhance corrosion resistance. This suggests that although the value established by standards may optimize improvements in mechanical parameters, such as the yield strength, ultimate strength, and toughness of the steel, it may not necessarily yield the best durability performance when the steel is exposed to corrosive atmospheres.
- The addition of niobium to steel consistently enhances its corrosion resistance across various types of corrosive atmospheres. This improvement is attributed to the formation of a compact layer of niobium oxides that shields the steel from dissolution. However, it is crucial to monitor the quantity of niobium added, as excessive amounts (>1.0 wt.%) can result in the formation of Fe_2Nb, which actually increases the steel's susceptibility to corrosion.
- Generally, higher levels of corrosion result in significant reductions in the mechanical behavior of steel beams. This degradation is challenging to predict consistently due to the wide range of variables present in different studies. Moreover, corrosion influences the slenderness ratio of the flange and the web, which are critical factors in the structural design of steel members. This interconnectedness highlights how corrosion impacts not only the material strength but also the fundamental design parameters of steel structures.
- Incorporating Nb as a microalloy significantly enhances the properties of the HAZ, improving toughness, strength, and corrosion resistance. Additionally, Nb contributes to reducing the grain size in the HAZ and promotes the formation of acicular ferrite. This leads to improved fracture toughness and resistance to plastic deformation, demonstrating how Nb plays a multifaceted role in enhancing the overall performance of the material.

Author Contributions: A.V.B.: Conceptualization, Methodology, Validation, Investigation, Formal analysis, Writing—Original Draft, Visualization. C.A.B.T.: Conceptualization, Methodology, Validation, Investigation, Formal analysis, Writing—Original Draft, Visualization. R.M.d.C.S.: Conceptualization, Validation, Investigation, Formal analysis, Writing—Original Draft, Visualization. P.A.K.: Conceptualization, Resources, Supervision, Writing—Review and Editing. D.C.T.C.: Conceptualization, Resources, Supervision, Writing—Review and Editing. F.d.A.S.: Conceptualization, Resources, Supervision, Writing—Review and Editing. C.H.M.: Conceptualization, Resources, Supervision, Writing—Review and Editing, Project administration, Funding acquisition. All authors have read and agreed to the published version of the manuscript.

Funding: This study was financed in part by the Conselho Nacional de Desenvolvimento Científico e Tecnológico (CNPq) provided under Project No. 408498/2022-6 and the Coordenação de Aperfeiçoamento de Pessoal de Nível Superior—Brasil (CAPES)—Finance Code 001.

Conflicts of Interest: The authors declare no conflicts of interest.

Appendix A

Table A1. Experimental studies of niobium microalloyed steel beams subjected to corrosion.

Research	Span (m)	Steel Beam								Corrosion Method	Experimental Test	Mass Loss (%)	Failure Mode	Peak Load Reduction (%)
		Steel Nom.	f_y (MPa)	h (mm)	h_w (mm)	t_w (mm)	t_f (mm)	b_f (mm)	Nb Content					
Peng et al. [70]	1.8	Q460D	460	200	184	8	8	150	0.19	Immersion in a 5 wt.% NaCl solution. Corrosion current: 1880 mA	4-point bending test	0	local buckling of upper flange	0
												5	local buckling of upper flange	6.09
												10	local buckling of upper flange	13.41
												15	buckling of upper flange and web near mid-span	32.90
Zhang et al. [72]	1.5	Q345	345	200	182	6	9	150	$\leq$0.07 †	Outdoor artificial accelerated corrosion test up to 12 months	4-point bending test	0	local buckling of upper flange	0
												5.63	local buckling of upper flange	17.4
												6.89	buckling of upper flange and web near mid-span	21.71
												13.1	buckling of upper flange and web near mid-span	27.54
												16.88	buckling of upper flange and web near mid-span	30.5
Xiao et al. [74]	1.8	Q460D	460	200	184	8	8	150	0.19	Immersion in a 5 wt.% NaCl solution. Corrosion current: 0.005 mA/cm^2	4-point bending test	0	buckling of upper flange	0
												4.87	buckling of upper flange	2.83
												9.61	buckling of upper flange	12.97
												11.67	web buckling failure	30.89
												14.87	web buckling failure	64.15

[Note] f_y = yield strength, h = steel beam depth, h_w = web depth, t_w = web thickness, t_f = flange thickness, b_f = flange width, † According to GB/T 1591-2008 [101] standard.

References

1. Xie, H.; Du, L.; Hu, J.; Misra, R. Microstructure and mechanical properties of a novel 1000 MPa grade TMCP low carbon microalloyed steel with combination of high strength and excellent toughness. *Mater. Sci. Eng. A-Struct. Mater. Prop. Microstruct. Process.* **2014**, *612*, 123–130. [CrossRef]
2. Patterson, T.; Lippold, J. Effect of niobium on the microstructure and properties of submerged arc welds in HSLA steel. *Weld. World* **2020**, *64*, 1089–1105. [CrossRef]
3. Wu, W.; Wang, Q.; Yang, L.; Liu, Z.; Li, X.; Li, Y. Corrosion and SCC initiation behavior of low-alloy high-strength steels microalloyed with Nb and Sb in a simulated polluted marine atmosphere. *J. Mater. Res. Technol.* **2020**, *9*, 12976–12995. [CrossRef]
4. Zhao, Q.; Fan, E.; Wang, S.; Zhao, J.; Huang, Y.; Li, X. Understanding the Effect of Nanosized NbC Precipitates on the Stress Corrosion Cracking of High-Strength Low-Alloy Steel in a Simulated Deep-Sea Environment. *J. Mater. Eng. Perform.* **2021**, *30*, 2159–2173. [CrossRef]
5. Jia, J.; Cheng, X.; Yang, X.; Li, X.; Li, W. A study for corrosion behavior of a new-type weathering steel used in harsh marine environment. *Constr. Build. Mater.* **2020**, *259*, 119760. [CrossRef]
6. Yu, H.; Wu, K.; Dong, B.; Yu, L.; Liu, J.; Liu, Z.; Xiao, D.; Jing, X.; Liu, H. Effect of Niobium Content on the Microstructure and Mechanical Properties of Simulated Coarse-Grained Heat-Affected Zone (CGHAZ) of High-Strength Low-Alloy (HSLA) Steels. *Materials* **2022**, *15*, 3318. [CrossRef]
7. Villalobos, J.; Del-Pozo, A.; Campillo, B.; Mayen, J.; Serna, S. Microalloyed Steels through History until 2018: Review of Chemical Composition, Processing and Hydrogen Service. *Metals* **2018**, *8*, 351. [CrossRef]
8. Baker, T. Microalloyed steels. *Ironmak. Steelmak.* **2016**, *43*, 264–307. [CrossRef]
9. Liu, Z.G.; Wang, Y.M.; Zhai, Y.D.; Li, P.; Su, G.Q. Study on the role of niobium in corrosion mechanism of low-alloy pipeline steel in H2S-saturated solution. *Int. J. Hydrogen Energy* **2023**, *48*, 22192–22208. [CrossRef]
10. Zhang, C.; Hui, W.; Zhao, X.; Zhang, Y.; Zhao, X. The potential significance of microalloying with Nb in enhancing the resistance to hydrogen-induced delayed fracture of 1300-MPa-grade high-strength bolt steel. *Eng. Fail. Anal.* **2022**, *135*, 106–144. [CrossRef]
11. Tian, S.; Liu, Z.; Fu, R.; Wang, X. Effect of niobium alloying on the austenite grain growth and mechanical properties of ultrahigh-strength stainless steel. *Mater. Res. Express* **2022**, *9*, 026511. [CrossRef]
12. Liu, X.; Wang, H.; Liu, Y.; Wang, C.; Song, Q.; Cui, H.; Zhang, C.; Huang, K. The effect of Nb content on microstructure and properties of laser cladding 316L SS coating. *Surf. Coat. Technol.* **2021**, *425*, 127684. [CrossRef]
13. Qiao, Q.; Lu, L.; Fan, E.; Zhao, J.; Liu, Y.; Peng, G.; Huang, Y.; Li, X. Effects of Nb on stress corrosion cracking of high-strength low-alloy steel in simulated seawater. *Int. J. Hydrogen Energy* **2019**, *44*, 27962–27973. [CrossRef]
14. Hutchinson, C.; Zurob, H.; Sinclair, C.; Brechet, Y. The comparative effectiveness of Nb solute and NbC precipitates at impeding grain-boundary motion in Nb steels. *Scr. Mater.* **2008**, *59*, 635–637. [CrossRef]
15. Sun, L.; Liu, X.; Xu, X.; Lei, S.; Li, H.; Zhai, Q. Review on niobium application in microalloyed steel. *J. Iron Steel Res. Int.* **2022**, *29*, 1513–1525. [CrossRef]
16. Jack, T.; Szpunar, J. Effect of Nb-induced microstructure on pipeline steel corrosion and stress corrosion cracking performance in acidic environment. *Corros. Sci.* **2023**, *218*, 111196. [CrossRef]
17. Nam, N.; Kim, J. Effect of niobium on the corrosion behaviour of low alloy steel in sulfuric acid solution. *Corros. Sci.* **2010**, *52*, 3377–3384. [CrossRef]
18. Ardila, M.; Labiapari, W.; de Mello, J. The Influence of Crystallographic Texture and Niobium Stabilisation on the Corrosion Resistance of Ferritic Stainless Steel. *Mater. Res.-Ibero-Am. J. Mater.* **2017**, *20*, 576–583. [CrossRef]
19. Wang, Z.; Wu, J.; Li, J.; Wu, X.; Huang, Y.; Li, X. Effects of Niobium on the Mechanical Properties and Corrosion Behavior of Simulated Weld HAZ of HSLA Steel. *Metall. Mater. Trans. A-Phys. Metall. Mater. Sci.* **2018**, *49*, 187–197. [CrossRef]
20. Fernandez, J.; Illescas, S.; Guilemany, J. Effect of microalloying elements on the austenitic grain growth in a low carbon HSLA steel. *Mater. Lett.* **2007**, *61*, 2389–2392. [CrossRef]
21. Mandal, P.; Kant, R. Effect of microalloying elements on mechanical properties in the high strength low alloy steel. *Mater. Sci. Forum* **2015**, *830–831*, 231–233. [CrossRef]
22. Orban, M.; Palfalvi, A. A Comparative Study of the Possibilities of B. Nb, Ti and V Using as Microalloying Elements in PM Steels Strengthening. *Microstruct. Investig. Anal.* **2000**, *4*, 248–251. [CrossRef]
23. Bu, F.; Wang, X.; Yang, S.; Shang, C.; Misra, R. Contribution of interphase precipitation on yield strength in thermomechanically simulated Ti-Nb and Ti-Nb-Mo microalloyed steels. *Mater. Sci. Eng. A-Struct. Mater. Prop. Microstruct. Process.* **2015**, *620*, 22–29. [CrossRef]
24. Gu, Y.; Qiao, G.; Wu, D.; Liao, B.; Xiao, F. Precipitation kinetics of Nb carbonitride in austenite and acicular ferrite and its effect on hardness of high-Nb steel. *Mater. Chem. Phys.* **2016**, *183*, 506–515. [CrossRef]
25. Massey, C.; Hoelzer, D.; Seibert, R.; Edmondson, P.; Kini, A.; Gault, B.; Terrani, K.; Zinkle, S. Microstructural evaluation of a Fe-12Cr nanostructured ferritic alloy designed for impurity sequestration. *J. Nucl. Mater.* **2019**, *522*, 111–122. [CrossRef]
26. Rancel, L.; Gomez, M.; Medina, S. Influence of Microalloying Elements (Nb, V, Ti) on Yield Strength in Bainitic Steels. *Steel Res. Int.* **2008**, *79*, 947–953. [CrossRef]
27. Callister, W.; Rethwisch, D. *Materials Science and Engineering: An Introduction*, 9th ed.; John Wiley & Sons: Hoboken, NJ, USA, 2013.
28. Calhoun, R.; Dunand, C. Dislocations in Metal Matrix Composites: Metal Matrix Composites. In *Comprehensive Composite Materials: Metal Matrix Composites*; Elsevier: Amsterdam, The Netherlands, 2000; pp. 27–59. [CrossRef]

29. Ke, R.; Hu, C.; Zhong, M.; Wan, X.; Wu, K. Grain refinement strengthening mechanism of an austenitic stainless steel: Critically analyze the impacts of grain interior and grain boundary. *J. Mater. Res. Technol.* **2022**, *17*, 2999–3012. [CrossRef]
30. Antonov, S.; Detrois, M.; Tin, S. Design of Novel Precipitate-Strengthened Al-Co-Cr-Fe-Nb-Ni High-Entropy Superalloys. *Metall. Mater. Trans. A-Phys. Metall. Mater. Sci.* **2018**, *49*, 305–320. [CrossRef]
31. Abdullah, B.; Alias, S.K.; Jaffar, A.; Rashid, A.A.; Ramli, A. Mechanical properties and microstructure analysis of 0.5% Niobium alloyed ductile iron under austempered process in salt bath treatment. In Proceedings of the International Conference on Mechanical and Electrical Technology, Singapore, 10–12 September 2010; IEEE: Piscataway, NJ, USA, 2010; pp. 610–614. [CrossRef]
32. Bai, G.; Lu, S.; Li, D.; Li, Y. Influences of niobium and solution treatment temperature on pitting corrosion behaviour of stabilised austenitic stainless steels. *Corros. Sci.* **2016**, *108*, 111–124. [CrossRef]
33. Wu, S.; Zhang, C.; Zhang, S.; Wang, Q.; Liu, Y.; Abdullah, A. Effect of Nb addition on microstructure and corrosion resistance of novel stainless steels fabricated by direct laser metal deposition. *Mater. Res. Express* **2018**, *5*, 036524. [CrossRef]
34. Yu, H.; Wu, K.; Dong, B.; Liu, J.; Liu, Z.; Xiao, D.; Jin, X.; Liu, H.; Tai, M. Effect of Heat-Input on Microstructure and Toughness of CGHAZ in a High-Nb-Content Microalloyed HSLA Steel. *Materials* **2022**, *15*, 3588. [CrossRef] [PubMed]
35. Raj, B.; Jappes, J.; Khan, M.; Dillibabu, V.; Brintha, N. Studies on heat treatment and electrochemical behaviour of 3D printed DMLS processed nickel-based superalloy. *Appl. Phys. A-Mater. Sci. Process.* **2019**, *125*, 722. [CrossRef]
36. Zhang, X.; Wei, W.; Cheng, L.; Liu, J.; Wu, K.; Liu, M. Effects of niobium and rare earth elements on microstructure and initial marine corrosion behavior of low-alloy steels. *Appl. Surf. Sci.* **2019**, *475*, 83–93. [CrossRef]
37. Fu, J.; Wang, J.; Li, F.; Cui, K.; Du, X.; Wu, Y. Effect of Nb addition on the microstructure and corrosion resistance of ferritic stainless steel. *Appl. Phys. A-Mater. Sci. Process.* **2020**, *126*, 194. [CrossRef]
38. Hajsman, J.; Kucerova, L.; Burdova, K. The Influence of Varying Aluminium and Manganese Content on the Corrosion Resistance and Mechanical Properties of High Strength Steels. *Metals* **2021**, *11*, 1446. [CrossRef]
39. Moradi, S.; Zangeneh, S.; Vardak, S.; Bahrami, R. New Co-Cr-Mo-Nb-Cu alloy for implant applications: Properties characterization. *J. Alloys Compd.* **2022**, *925*, 166387. [CrossRef]
40. Wu, W.; Liu, Z.; Wang, Q.; Li, X. Improving the resistance of high-strength steel to SCC in a SO2-polluted marine atmosphere through Nb and Sb microalloying. *Corros. Sci.* **2020**, *170*, 108693. [CrossRef]
41. Zong, Y.; Liu, C. Microstructure, mechanical properties, and Corrosion Behavior of Ultra-Low Carbon Bainite Steel with Different Niobium Content. *Materials* **2021**, *14*, 311. [CrossRef]
42. Xu, X.; Wu, W.; Li, N.; Zhang, L.; Wang, Y.; Liu, Z.; Li, X. Effect of 0.1 wt% Nb on the microstructure and corrosion fatigue performance of high strength steels. *Corros. Sci.* **2023**, *219*, 111242. [CrossRef]
43. Zhao, P.; Liu, Z.; Du, F.; Misra, R.; Zhang, C.; Zhou, X.; Yan, E. Ultra-high cycle fatigue property of a multiphase steel microalloyed with niobium. *Mater. Sci. Eng. A-Struct. Mater. Prop. Microstruct. Process.* **2018**, *718*, 1–8. [CrossRef]
44. Zhao, P.; Cheng, C.; Gao, G.; Hui, W.; Misra, R.; Bai, B.; Weng, Y. The potential significance of microalloying with niobium in governing very high cycle fatigue behavior of bainite/martensite multiphase steels. *Mater. Sci. Eng. A-Struct. Mater. Prop. Microstruct. Process.* **2016**, *650*, 438–444. [CrossRef]
45. Lima, C.; Belém, M.; Camargo, F. Analysis of Mechanical and Tribocorrosion Properties of Thermally Sprayed Nb2O5 Coatings. In Proceedings of the International Thermal Spray Conference (ITSC2018), Orlando, FL, USA, 7–10 May 2018; pp. 781–786.
46. Liu, S.; Gao, C.; Yan, P. Effect of Niobium Micro-Alloying Addition on Electrochemical Corrosion Behavior of Mild Steel in a Highly Alkaline Environment. *Int. J. Electrochem. Sci.* **2020**, *15*, 5333–5341. [CrossRef]
47. Li, J.; Wu, J.; Wang, Z.; Zhang, S.; Wu, X.; Huang, Y.; Li, X. The effect of nanosized NbC precipitates on electrochemical corrosion behavior of high strength low -alloy steel in 3.5%NaCl solution. *Int. J. Hydrogen Energy* **2017**, *42*, 22175–22184. [CrossRef]
48. Tzortzinis, G.; Knickle, B.; Bardow, A.; Brena, S.; Gerasimidis, S. Strength evaluation of deteriorated girder ends. I: Experimental study on naturally corroded I-beams. *Thin-Walled Struct.* **2021**, *159*, 107220. [CrossRef]
49. Inkscape Project. Inkscape Version 1.3 [Internet]. 2020. Available online: https://inkscape.org (accessed on 15 January 2024).
50. Tzortzinis, G.; Ai, C.; Brena, S.; Gerasimidis, S. Using 3D laser scanning for estimating the capacity of corroded steel bridge girders: Experiments, computations and analytical solutions. *Eng. Struct.* **2022**, *265*, 114407. [CrossRef]
51. Wang, Y.; Xu, S.; Li, A. Flexural performance evaluation of corroded steel beams based on 3D corrosion morphology. *Struct. Infrastruct. Eng.* **2020**, *16*, 1562–1577. [CrossRef]
52. Kuang, Y.; Feng, J.; Yu, Z.; Liu, X. Experimental study and analysis of the structural behavior of steel-concrete composite beam after shear connector corrosion. *Appl. Mech. Mater.* **2014**, *578–579*, 1522–1530. [CrossRef]
53. Sheng, J.; Xia, J.; Ma, R. Experimental study on the coupling effect of sulfate corrosion and loading on the mechanical behavior of steel and H-section beam. *Constr. Build. Mater.* **2018**, *189*, 711–718. [CrossRef]
54. Chen, J.; Zhang, H.; Yu, Q. Monotonic and fatigue behavior of steel-concrete composite beams subjected to corrosion. *Structures* **2021**, *34*, 1973–1984. [CrossRef]
55. Luo, L.; Fu, H.; Zhang, Y.; Xie, X. Experimental Study on the Overall Stability of Corroded H-Shaped Steel Beams. *Buildings* **2022**, *12*, 1923. [CrossRef]
56. Nie, B.; Xu, S.; Zhang, Z.; Gu, R. Experimental investigation on corroded cold-formed steel beam-columns under compression and major axis bending. *J. Constr. Steel Res.* **2020**, *169*, 106026. [CrossRef]
57. Wang, B.; Huang, W.; Zheng, S. Study on Restoring Force Performance of Corrosion Damage Steel Frame Beams under Acid Atmosphere. *Appl. Sci.* **2019**, *9*, 103. [CrossRef]

58. Wang, H.; Wang, Y.; Zhang, Z.; Liu, X.; Xu, S. Cyclic behavior and hysteresis model of beam-column joint under salt spray corrosion environment. *J. Constr. Steel Res.* **2021**, *183*, 106737. [CrossRef]
59. Wang, Y.; Shi, T.; Ma, R.; Xu, S. Experimental study on seismic performance of H-section beam-column welded connections corroded in general atmosphere. *J. Build. Struct.* **2022**, *43*, 184. [CrossRef]
60. Zhang, X.; Zheng, S.; Zhao, X. Experimental and numerical investigations into seismic behavior of corroded steel frame beams and columns in offshore atmospheric environment. *J. Constr. Steel Res.* **2023**, *201*, 107757. [CrossRef]
61. Zhang, X.; Zheng, S.; Zhao, X. Experimental and numerical study on seismic performance of corroded steel frames in chloride environment. *J. Constr. Steel Res.* **2020**, *171*, 106164. [CrossRef]
62. Xiao, L.; Peng, J.; Zhang, J.; Cai, C. Experimental investigation and numerical analysis on stiffness degradation of high-performance steel beams with local shear-span corrosion. *Earth Space* **2021**, *2021*, 533–541. [CrossRef]
63. Bao, A.; Guillaume, C.; Satter, C.; Moraes, A.; Williams, P.; Kelly, T.; Guo, Y. Testing and evaluation of web bearing capacity of corroded steel bridge girders. *Eng. Struct.* **2021**, *238*, 112276. [CrossRef]
64. Zakowski, K.; Narozny, M.; Szocinski, M.; Darowicki, K. Influence of water salinity on corrosion risk-the case of the southern Baltic Sea coast. *Environ. Monit. Assess.* **2014**, *186*, 4871–4879. [CrossRef]
65. Zhu, J.; Li, D.; Chang, W.; Wang, Z.; Hu, L.; Zhang, Y.; Wang, M.; Yang, Z.; Song, J.; Chen, S.; et al. In situ marine exposure study on corrosion behaviors of five alloys in coastal waters of western Pacific Ocean. *J. Mater. Res. Technol.* **2020**, *9*, 8104–8116. [CrossRef]
66. Morcillo, M.; Chico, B.; Diaz, I.; Cano, H.; de la Fuente, D. Atmospheric corrosion data of weathering steels. A review. *Corros. Sci.* **2013**, *77*, 6–24. [CrossRef]
67. *ISO 9223:2012*; Corrosion of Metals and Alloys, Corrosivity of Atmospheres, Classification, Determination and Estimation. ISO: Geneva, Switzerland, 2022; p. 15.
68. Ranji, A.R.; Zakeri, S. Mechanical properties and corrosion resistance of normal strength and high strength steels in chloride solution. In Proceedings of the Corrosion 2011, Houston, TX, USA, 13–17 March 2011. [CrossRef]
69. Chen, J.; Jiang, A.; Jin, W. Behavior of Steel–Concrete Composite Beams with Corroded Shear Studs Under Negative Bending Moment. In Proceedings of the 4th International Conference on the Durability of Concrete Structures, West Lafayette, IN, USA, 24–26 July 2014; pp. 127–136. [CrossRef]
70. Peng, J.; Xiao, L.; Zhang, J.; Cai, C.; Wang, L. Flexural behavior of corroded HPS beams. *Eng. Struct.* **2019**, *195*, 274–287. [CrossRef]
71. Drazic, D.; Vasciz, V. The correlation between accelerated laboratory corrosion tests and atmospheric corrosion station tests on steels. *Corros. Sci.* **1989**, *29*, 1197–1204. [CrossRef]
72. Zhang, Z.; Xu, S.; Wang, H.; Nie, B.; Su, C. Flexural buckling behavior of corroded hot-rolled H-section steel beams. *Eng. Struct.* **2021**, *229*, 111614. [CrossRef]
73. Sheng, J.; Xia, J.; Chang, H. Bending Behavior of Corroded H-Shaped Steel Beam in Underground Environment. *Appl. Sci.* **2021**, *11*, 938. [CrossRef]
74. Xiao, L.; Peng, J.; Cai, C.; Chen, H. Experimental and numerical investigations on the mechanical behavior of coastal high performance steel beams with local corrosion within the shear-span. *Appl. Ocean Res.* **2023**, *136*, 103581. [CrossRef]
75. Ma, H.; Zhao, J.; Fan, Y.; Huang, Y.; Liu, Z.; Du, C.; Li, X. Comparative study on corrosion fatigue behaviour of high strength low alloy steel and simulated HAZ microstructures in a simulated marine atmosphere. *Int. J. Fatigue* **2020**, *137*, 105666. [CrossRef]
76. Guo, Y.; Shao, Y.; Gao, X.; Li, T.; Zhong, Y.; Luo, X. Corrosion fatigue crack growth of serviced API 5L X56 submarine pipeline. *Ocean Eng.* **2022**, *256*, 111502.
77. Zhou, X.; Zhang, X.; Xu, R.; Li, B.; Ren, X.; Zhu, J.; Jin, Y. Galvanic Corrosion and Fatigue Behavior of a *SM*480C Welded Joint Steel in a Sea-Crossing Suspension Bridge. *Int. J. Corros.* **2022**, *2022*, 2665663. [CrossRef]
78. Ashby, M.; Easterling, K. The transformation hardening of steel surfaces by laser beams—I. Hypo-eutectoid steels. *Acta Metall.* **1984**, *32*, 1935–1948. [CrossRef]
79. Bhadeshia, H.; Honeycombe, R. *Steels: Microstructure and Properties*, 3rd ed.; Butterworth-Heinemann: Oxford, UK, 2006.
80. Radaj, D.; Sonsino, C.; Fricke, W. *Fatigue Assessment of Welded Joints by Local Approaches*, 2nd ed.; Woodhead Publishing: Sawston, UK, 2006. [CrossRef]
81. Barbaro, F.; Kuzmikova, L.; Zhu, Z.; Li, H. Weld Haz Properties in Modern High Strength Niobium Pipeline Steels. In *Energy Materials 2014: Conference Proceedings*; Springer International Publishing: Cham, Switzerland, 2016; pp. 657–664. [CrossRef]
82. David, S.; Debroy, T. Current issues and problems in welding science. *Science* **1992**, *257*, 497–502. [CrossRef] [PubMed]
83. Zhao, T.; Liu, Z.; Hu, S.; Du, C.; Li, X. Effect of Hydrogen Charging on the Stress Corrosion Behavior of 2205 Duplex Stainless Steel Under 3.5 wt.% NaCl Thin Electrolyte Layer. *J. Mater. Eng. Perform.* **2017**, *26*, 2837–2846. [CrossRef]
84. Zhou, Y.; Jia, T.; Zhang, X.; Liu, Z.; Misra, R. Microstructure and toughness of the CGHAZ of an offshore platform steel. *J. Mater. Process. Technol.* **2015**, *219*, 314–320. [CrossRef]
85. Yan, W.; Luo, X.; Xu, G.; Wang, H.; Wang, Z.; Chen, X. Significant improvement in CGHAZ toughness of HSLA steel via welding with trailing mechanical treatment. *Mater. Sci. Eng. A-Struct. Mater. Prop. Microstruct. Process.* **2022**, *837*, 142725. [CrossRef]
86. Liang, G.; Yang, S.; Wu, H.; Liu, X. Microstructure and mechanical performances of CGHAZ for oil tank steel during high heat input welding. *Rare Met.* **2013**, *32*, 129–133. [CrossRef]
87. Cao, X.; Zhou, X.; Wang, H.; Luo, Z.; Duan, J. Microstructures and mechanical properties of laser offset welded 5052 aluminum to press-hardened steel. *J. Mater. Res. Technol.* **2020**, *9*, 5378–5390. [CrossRef]

88. Sun, M.; Wang, Z.; Wang, X.; Misra, R. The significance of variant pairing in governing toughness of coarse-grained heat affected zone (CGHAZ) in Nb-bearing high strength structural steels. *Mater. Lett.* **2020**, *260*, 126974. [CrossRef]
89. Li, Y.; Baker, T. Effect of morphology of martensite-austenite phase on fracture of weld heat affected zone in vanadium and niobium microalloyed steels. *Mater. Sci. Technol.* **2010**, *26*, 1029–1040. [CrossRef]
90. Jha, R.; Bhuyan, P.; Mandal, S.; Pal, S. Insights into the role of Nb segregation on grain boundary structural transition and mechanical response in a Ni-Nb system. *Mater. Chem. Phys.* **2023**, *299*, 127531. [CrossRef]
91. Mha, P.; Tongne, A.; Pantalé, O. A generalized non-linear flow law based on modified Zerilli-Armstrong model and its implementation into Abaqus/Explicit FEM Code. *World J. Eng. Technol.* **2022**, *10*, 334–362. [CrossRef]
92. *ASTM E23-12a*; Standard Test Methods for Notched Bar Impact Testing of Metallic Materials. ASTM: West Conshohocken, PA, USA, 2013; p. 24.
93. *BS EN 10045-1:1990*; Charpy Impact Test on Metallic Materials. Test Method (V- and U-Notches). BSI: Brussels, Belgium, 2007; p. 14.
94. Jegdić, B.; Bobić, B.; Bošnjakov, M.; Alić, B. Testing of intergranular and pitting corrosion in sensitized welded joints of austenitic stainless steel. *Metall. Mater. Eng.* **2017**, *23*, 109–117. [CrossRef] [PubMed]
95. *ASTM G5-14*; Standard Reference Test Method for Making Potentiodynamic Anodic Polarization Measurements. ASTM: West Conshohocken, PA, USA, 2021; p. 9.
96. *ASTM G59-23*; Standard Test Method for Conducting Potentiodynamic Polarization Resistance Measurements. ASTM: West Conshohocken, PA, USA, 2023; p. 4.
97. *ASTM G102-23*; Standard Practice for Calculation of Corrosion Rates and Related Information from Electrochemical Measurements. ASTM: West Conshohocken, PA, USA, 2023; p. 8.
98. Zhu, Y.; Ma, J.; Wang, G.; Song, K.; Stock, H. Corrosion behaviour of multilayer CrN coatings deposited by hybrid HIPIMS after oxidation treatment. *Nanotechnol. Rev.* **2020**, *9*, 596–609. [CrossRef]
99. Kaiser, M.; Qadir, M. Electrochemical corrosion performance of commercially used aluminium engine block and piston in 0.1 m NaCl. *J. Mech. Eng.* **2015**, *45*, 48–52. [CrossRef]
100. Wu, X.; Li, L.; Li, H.; Li, B.; Ling, Z. Effect of strain level on corrosion of stainless steel bar. *Constr. Build. Mater.* **2018**, *163*, 189–199. [CrossRef]
101. *GB/T 1591-2008*; High Strength Low Alloy Structural Steels. State Administration of Technical Supervision and Inspection: Beijing, China, 2008. (In Chinese)